Trade-offs and selection conflicts in hybrid poplars indicate the stomatal ratio as an important trait regulating disease resistance.

Karl C. Fetter[a], David M. Nelson[b], Stephen R. Keller[a]

[a]Department of Plant Biology, University of Vermont

[b]Appalachian Laboratory, University of Maryland Center for Environmental Science

Corresponding authors: Karl C. Fetter (e-mail: kf@uvm.edu)

Stephen R. Keller (e-mail: srkeller@uvm.edu, tel: +1 802 656 2930).

ABSTRACT Natural selection can remove maladaptive genotypic variance from populations, leaving reduced phenotypic variation as a signal of its action. Hybrid populations offer a unique opportunity to study phenotypic variance before selection purifies it, as these populations can have increased genotypic and phenotypic variance than can reveal trade-offs and selection conflicts not visible, or visible to a lesser extent, in unadmixed populations. Here, we study the interactions between a fungal leaf rust disease (*Melampsora medusae*) and stomata and ecophysiology traits in a set of hybrid and unadmixed individuals formed by natural matings between *Populus balsamifera*, *P. trichocarpa*, *P. angustifolia*, and *P. deltoides*. Phenotypes were measured on cloned genotypes grown in a common garden and genotyped at 227K SNPs with GBS. Our analyses indicate hybridization decreases disease resistance and increases the variance of stomatal ratio (SR), or the ratio of upper leaf surface stomata density to total stomata density. Heritability of SR was high in admixed populations ($H^2 = 0.72$) and covaries strongly with the proportion of *P. balsamifera* ancestry in a genome; thus, selection could effectively reduce disease by selecting for low values of stomatal ratio. However, selection conflicts present in some admixed populations may prevent adaptation to pathogens as a result of these populations being unable to occupy adaptive trait space along the growth-defense spectrum. These results suggest an important role for SR and stomatal patterning traits as a target of pathogen induced selection to achieve local fitness optima. Additionally, we demonstrate that hybridization is capable of generating, or magnifying maladaptive intermediate phenotypes to reveal trade-offs and selection conflicts.

INDEX TERMS Hybridization, trade-offs, selection conflicts, *Populus*, *Melampsora*, plant pathology.

ABSTRACT

Natural selection can remove maladaptive genotypic variance from populations, leaving reduced phenotypic variation as a signal of its action. Hybrid populations offer a unique opportunity to study phenotypic variance before selection purifies it, as these populations can have increased genotypic and phenotypic variance than can reveal trade-offs and selection conflicts not visible, or visible to a lesser extent, in unadmixed populations. Here, we study the interactions between a fungal leaf rust disease (*Melampsora medusae*) and stomata and ecophysiology traits in a set of hybrid and unadmixed individuals formed by natural matings between *Populus balsamifera*, *P. trichocarpa*, *P. angustifolia*, and *P. deltoides*. Phenotypes were measured on cloned genotypes grown in a common garden and genotyped at 227K SNPs with GBS. Our analyses indicate hybridization decreases disease resistance and increases the variance of stomatal ratio (SR), or the ratio of upper leaf surface stomata density to total stomata density. Heritability of SR was high in admixed populations ($H^2 = 0.72$) and covaries strongly with the proportion of *P. balsamifera* ancestry in a genome; thus, selection could effectively reduce disease by selecting for low values of stomatal ratio. However, selection conflicts present in some admixed populations may prevent adaptation to pathogens as a result of these populations being unable to occupy adaptive trait space along the growth-defense spectrum. These results suggest an important role for SR and stomatal patterning traits as a target of pathogen induced selection to achieve local fitness optima. Additionally, we demonstrate that hybridization is capable of generating, or magnifying maladaptive intermediate phenotypes to reveal trade-offs and selection conflicts.

I. INTRODUCTION

Trade-offs arise when selection on fitness components is constrained by negative correlations between pairs of traits (Stearns, 1989; Schluter et al., 1991). In plants, an important life history trade-off is between size and the age of first reproduction, with delayed reproduction correlating with longer fertility and higher quality offspring that have a greater chance of survival (Stearns, 1989). However, plants must cope with numerous natural enemies (e.g. herbivores and pathogens), and delaying reproduction can come at a high cost if diverting limited resources to defense away from reproduction reduces fitness (Obeso, 2002). Depending on pathogen prevalence, plant life histories generally evolve towards increased investment in defensive enzymes and compounds paired with slower growth, or decreased investment in defense paired with faster growth. The fast-slow trade-off has been consistently identified in annuals (Tian et al., 2003), perennials (Messina et al., 2002), and long-lived trees (McKown et al., 2014; McKown et al., 2019), although this hypothesis is not without its critics (Kliebenstein, 2016).

At the molecular level, the plant growth-defense trade-off is regulated by cellular signaling and hormonal regulation to direct metabolic activity away from growth and towards defense, or vice versa (Tian et al., 2003; Wang, 2012; Chandran et al., 2014). Host plant species may evolve a variety of costly defenses to combat disease, including the evolution of structural phenotypes to reduce exposure to pathogens (Gonzales-Vigil et al., 2017), immune systems to detect pathogens (Dangl and Jones, 2001) in order to initiate appropriate responses (Cai et al., 2018), and resistance via constitutive or inducible synthesis of defensive compounds (Bailey et al., 2005; Ullah et al., 2018). Hosts may also avoid disease by migrating out of environments where a pathogen spatially or temporally occurs (Altizer et al., 2011), by colonizing new environments where the pathogen is absent (Bruns et al., 2018), or by evolving life history strategies that avoid or compensate for pathogen exposure (Stearns, 1989).

The phenotypic expression of growth-defense trade-offs may be altered by hybridization between parental species that have evolved different strategies of growth or defense. Hybridization is an important mechanism for evolutionary change, and has been implicated in the maintenance of species boundaries due to negative selection on advanced generation hybrids (Christe et al., 2016), introgression of beneficial alleles across species barriers (Chhatre et al., 2018), and, among other evolutionary phenomena, speciation (Mallet, 2007). It is well-known that hybridization changes the mean and variance of traits in hybrid populations with regards to either parental species; indeed, crop breeders intentionally create hybrids to take advantage of hybrid vigor and transgressive segregation in F_1 hybrids to increase yields and select for novel phenotypic combinations (Goulet et al., 2017). Transgressive segregation in hybrids is a source of new phenotypes for selection to act upon in natural populations (Goulet et al., 2017), and the balance between competing fitness components underlying trade-offs can change in hybrid populations (Ellstrand and Schierenbeck, 2000). For example, hybrid *Salix eriocephala* x *sericea* have an increase in disease severity to willow leaf rust (*Melampsora* sp.) by a factor of 3.5 in comparison to unadmixed parents (Roche and Fritz, 1998). Thus, it is apparent that hybridization can have beneficial and deleterious effects on fitness, but the role of hybridization in revealing fitness trade-offs that are not evident, or cryptic, within the parental species has been little explored.

One scenario where a trade-off between plant growth and defense may arise is the relationship between stomatal traits and infection by fungal pathogens. Stomata are microscopic valves on the surface of the leaf that regulate gas exchange during photosynthesis. Some foliar pathogens enter their hosts via stoma by sensing the topography of the leaf surface for guard

cells, and forming an appressorium over a stoma from which a penetration peg is used to invade the mesophyll tissue (Allen et al., 1991). The plant immune system has evolved mechanisms for detecting pathogens which can activate signal transduction pathways that lead stomatal closure (Melotto et al., 2006). However, closing stomata comes at the expense of limiting gas exchange, which may have negative effects on carbon assimilation depending on the water-use efficiency of photosynthesis. Thus, the conditions for the evolution of a growth-defense trade-off mediated by selection on stomata exists. Hybridization may be expected to shift genotypes along the trade-off continuum, and when competing strategies inherited from either parent meet in a hybrid, we may expect a mismatch between the optimal survival and growth strategy to result in increased disease.

In this study, we test for the effects of hybridization on disease severity and stomatal related growth traits, and investigate if hybridization reveals trade-offs and selection conflicts that may be masked in unadmixed populations. We use a sample of naturally formed hybrid genotypes between North American poplars infected by a common leaf rust of poplars, *Melampsora medusae*. We specifically ask the following questions: 1) how does hybridization change trait distributions, and does it alter their heritable variation; 2) which traits correlate most strongly with disease severity; 3) are there selection trade-offs between growth, disease severity, and stomatal traits; and 4) does hybridization reveal selection conflicts between traits underlying growth and defense?

II. MATERIALS & METHODS

A. STUDY SYSTEM

Poplars (*Populus*) are a genus of predominantly holarctic tree species (DiFazio et al., 2011). Extensive hybridization between species within a section of the genus, as well as between some sections, make the taxonomy of the genus difficult (Eckenwalder, 1996), with some authors identifying 29 (Eckenwalder, 1996) to as many as 60 species (Raven and Wu, 1999). Hybrids can be formed from species pairs within and between *Populus* sections *Tacamahaca* and *Aigeiros*, and extensive hybrid zones spontaneously form where the ranges of two reproductively compatible species meet (Suarez-Gonzalez et al., 2018c). Western North America contains several well documented hybrid zones (Martinsen et al., 2001; LeBoldus et al., 2013; Chhatre et al., 2018; Suarez-Gonzalez et al., 2018b), including a tri-hybdrid zone in Alberta, Canada (Floate et al., 2016). In this study, we work with hybrids formed from crosses between the section *Tacamahaca* species balsam poplar (*P. balsamifera*), and either a black balsam poplar (*P. trichocapra*), a narrow-leaf cottonwood (*P. angustifolia*), or an eastern cottonwood (*P. deltoides*) from the *Populus* section *Aigeiros*. We lack information on the which species served as the maternal vs. paternal parent for each hybrid, so we adopt the convention of listing the *P. balsamifera* parent first.

The disease we study is from the fungal leaf pathogen *Melampsora medusae*, a macrocyclic basidiomycete whose aecial host is a larch (*Larix*), and telial host is a poplar (Feau et al., 2007). Uredospores (N + N) of *M. medusae* can clonally reproduce on poplar leaves within a single season, and the closely related *M. larici-populina* is an agricultural pest that can reduce yields of hybrid poplars grown for agroforestry (Pinon and Frey, 2005).

B. MATERIALS

During winter 2013, dormant stem cuttings were collected from 534 trees from 59 populations spanning 9 Canadian provinces and 7 US States (longitudes -55 to -128 °W and latitudes 39 to 60 °N; Fig. 1, Table S1). The main focus of the 2013 collection was to sample *P. balsamifera* cuttings, but as the trees were dormant and some of the diagnostic traits were not immediately visible, a number of putative hybrids were also collected. Additionaly, 32 presumably unadmixed eastern cottonwood (*P. deltoides*) genotypes were collected in central Vermont, USA to serve as a reference population for identifying admixed *P. deltoides* hybrids with population genetic methods. For the 2013 collection, cuttings were grown for one year in a greenhouse, and then planted in the summer of 2014 in a common garden near Burlington, VT (44.444422 °N, -73.190164 °W). Replicates were planted in a randomized design with 2x2 meter spacing and 1,000 ramets were planted. The minimum, median, and maximum number of ramets per genet was 1, 2, and 6, respectively. Plants were not fertilized, but were irrigated as-needed during the 2014 growing season to ensure establishment, and then received no supplemental water.

C. MOLECULAR ANALYSES

Fresh foliage from greenhouse grown plants was used for extracting whole genomic DNA using DNeasy 96 Plant Mini Kits (Qiagen, Valencia, CA, USA). DNA was quantified using a fluorometric assay (Qubit BR, Invitrogen) and confirmed for high molecular weight using 1% agarose gel electrophoresis. We used genotyping-by-sequencing (GBS) (Elshire et al., 2011) to obtain genome-wide polymorphism data for all 534 trees. Genomic sequencing libraries were prepared from 100 ng of genomic DNA per sample digested with EcoT221 followed by ligation of barcoded adapters of varying length from 4-8 bp, following Elshire et al. (2011). Equimolar concentrations of barcoded fragments were pooled and purified with QIAquick PCR purification kit. Purified products were amplified with 18 PCR cycles to append Illumina sequencing primers, cleaned again using a PCR purification kit. The resulting library was screened for fragment size distribution using a Bioanalyzer. Libraries were sequenced at 48 plex (i.e., each library sequenced twice) using an Illumina HiSeq 2500 to generate 100 bp single end reads. Cornell University Institute of Genomic Diversity (Ithaca, NY) performed the library construction and sequencing steps. For the *P. deltoides* reference population, library preparation was performed using the same protocol. DNA sequencing was performed on an Illumina HiSeq 2500 at the Vermont Genetics Network core facility. Raw sequences reads are deposited in NCBI SRA under accession number SRP070954.

We employed the Tassel GBS Pipeline (Glaubitz et al., 2014) to process raw sequence reads and call variants and genotypes. In order to pass the quality control, sequence reads had to have perfect barcode matches, the presence of a restriction site overhang and no undecipherable nucleotides. Filtered reads were trimmed to 64 bp and aligned to the *P. trichocarpa* reference assembly version 3.0 (Tuskan et al., 2006) using the Burrows-Wheeler Aligner (BWA) (Li and Durbin, 2009). Single nucleotide polymorphisms (SNPs) were determined based on aligned positions to the reference, and genotypes called with maximum likelihood in Tassel (Glaubitz et al., 2014). SNP genotype and sequence quality scores were stored in Variant Call Format v4.1 (VCF) files, which were further processed with VCFTools 0.1.11 (Danecek et al., 2011). SNPs with a minor allele frequency < 0.001 were removed, and only biallelic sites were retained. Sites with with a mean depth < 5, genotype quality > 90, and indels

were removed. Missing data were imputed with Beagle v5.0 (Browning et al., 2018), and sites with post-imputation genotype probability < 90 and sites with any missingness were removed. After filtering, the final dataset contained 227,607 SNPs for downstream analyses.

The filial generation was estimated using NewHybrids (Anderson and Thompson, 2002) separately for each set of hybrids, (i.e. BxT, BxA, and BxD). Filial generation of *P. balsamifera* x *angustifolia* genotypes were previously estimated by Chhatre et al. (2018) and used here. NewHybrids requires reference populations for each species, and *P. trichocarpa* reference genotypes were downloaded from previously published work, and we selected 25 genotypes from Pierce Co, Washington in populations known to lack admixture with *P. balsamifera* (Evans et al., 2014). *P. deltoides* reference genotypes were collected from the Winooski and Mad River watersheds in central Vermont. The reference population for *P. balsamifera* was selected from individuals in the SLC, LON, and DPR populations that are known to lack admixture with other *Populus* species (see below). To select loci for distinguishing filial generations, we determined the locus-wise F_{ST} difference between reference populations. For the BxT analysis, 355 loci with an F_{ST} difference greater than 0.8 were randomly selected. In the BxD analysis, 385 loci that segregated completely between parental species (i.e. F_{ST} difference = 1) were randomly sampled. NewHybrids was run using Jeffrey's prior for π and θ for 200,000 sweeps with 100,000 discarded as burn-in. The cross type (BxB, BxT, BxA, or BxD) was determined from the NewHybrids result and the expected proportion of the genome from each parental species was calculated as:

$$\text{Expected ancestry proportion} = \frac{(2^n - 1)}{2^n}$$

where n = the number crossing events.

D. TRAIT MEASUREMENTS

All traits were measured from common garden grown trees in 2015, and disease severity was measured again in 2016 (Table 1). The severity of naturally innoculated leaf rust disease was phenotyped in both years using an ordinal scale from zero to four created by LaMantia et al. (2013) where: 0 = no uredinia visible, 1 = less than five uredinia per leaf on less than five leaves, 2 = less than five uredinia per leaf on more than five leaves, 3 = more than five uredinia per leaf on more than five leaves, and 4 = more than five uredinia on all leaves. In 2016, we also scored disease using the method of Dowkiw and Bastien (2004), where the single most infected leaf on a tree was classified as: 1 = no uredinia, 2 = 1 to 10 uredinia, 3 = 11 uredinia to 25 % of the leaf area, 4 = 25 to 50 % of the leaf area, 5 = 50 to 75 % of the leaf area, and 6 $\geq$ 75 % of the leaf area covered in uredinia. We refer to the ordinal scale of La Mantia et al. (2013) as ordinal scale 1 and the ordinal scale of Dowkiw and Bastien (2004) as ordinal scale 2. A mature larch tree (approx. 20m tall) was located approximately 100m from the garden site, and we assume a uniform distribution of aeciospore inoculum into the garden. The pathogen was visually confirmed to be *M. medusae* using microscopy to view the ellipsoid to obovoid shape of uredospores, the size range (min = 19.6 μ m, mean = 28.3 μ m, max = 34.45 μ m, N = 17, Fig. 1f), and the presence of a smooth equatorial region on the spore flanked by polar regions with papillae

(Van Kraayenoord et al., 1974) (Fig. 1f).

To collect isotopic, elemental, and specific leaf area (SLA) data, three hole punches (⌀= 3 mm) were sampled in June 2015 from a central portion of each leaf adjacent to, but avoiding the central leaf vein. Hole punches were dried at 65 °C to constant mass. Approximately 2 mg of foliar tissue from each sample was weighed into a tin capsule and analyzed for %C, %N, δ^{13}C, and δ^{15}N using a Carlo Erba NC2500 elemental analyzer (CE Instruments, Milano, Italy) interfaced with a ThermoFinnigan Delta V+ isotope ratio mass spectrometer (Bremen, Germany) at the Central Appalachians Stable Isotope Facility (CASIF) at the Appalachian Laboratory (Frostburg, Maryland, USA). %C and %N were calculated using a size series of atropine. The δ^{13}C and δ^{15}N data were normalized to the VPDB and AIR scales, respectively, using a two-point normalization curve with laboratory standards calibrated against USGS40 and USGS41. The long-term precision of an internal leaf standard analyzed alongside samples was 0.28‰ for δ^{13}C and 0.24‰ for δ^{15}N. Isotopic results are reported in units of per mil (‰). Carbon isotope discrimination against ^{13}C (Δ^{13}C) was calculated according to Farquhar et al. (1982) as:

$$\Delta^{13}C = (\delta^{13}C_{\text{a}} - \delta^{13}C_{\text{plant}})/(1 + \delta^{13}C_{\text{plant}})$$

where the $\delta^{13}C_a$ value (-8.456 ‰) was the mean value in 2015 measured at NOAA Mauna Loa observatory (White et al., 2011). Higher Δ^{13}C values indicate increased intracellular (C_{plant}) relative to atmospheric (C_a) CO_2 concentrations as a result of greater stomatal conductance and/or lower photosynthetic assimilation rates in C_3 plants. Δ^{13}C is a useful metric of intrinsic water use efficiency (ratio of photosynthesis to stomatal conductance) since both are influenced by C_i/C_a. We measured $delta^{15}$N as it is a measure of nitrogen demand within a plant given a uniform concentration of soil N (Craine et al., 2009). To calculate SLA, or the ratio of fresh punch area to dry leaf mass, three oven dried hole punches per leaf were massed collectively. Relative growth rate (G) was measured as the height increment gain (cm) between the apical bud in 2015 and the previous year's bud scar on the most dominant stem. The chlorophyll content index (CCI) was measured with a Konica Minolta SPAD 502 (Konica Minolta Sensing Americas, Inc) and the average of three measurements from the central portion of a leaf was recorded.

Stomata traits were measured from micrographs of nail polish casts sampled in 2014 from the abaxial (lower) and adaxial (upper) leaf surfaces. Leaves were collected from the field and placed in a cooler until processed in the lab. Nail polish peels were made and mounted on slides without a cover slip. Two non-overlapping areas without large veins from each peel were imaged (N = 1894) with an Olympus BX-60 microscope using differential interference contrast. Stomata density (SD) was estimated using the machine learning protocol of StomataCounter (Fetter et al., 2019). To verify the automatic counts, stomata were manually annotated on each image using the image annotation tool. The correlation between automatic and manual count was r = 0.99, and we used the automatic count data to calculate stomata density. To measure stomata pore length (PL), each image was segmented with four equally spaced horizontal lines in ImageJ (Schneider et al., 2012) and the length of a single pore was measured in each segmented region for a total of five observations per image. A measure of pore surface area, porosity, was calculated using the following formula: porosity = density * (π * (pore length / 2)^2). The stomata density ratio (SR), stomata pore length ratio (LR), and porosity ratio (PR) were calculated by dividing the value of the adaxial trait from the summed value

of the abaxial and adaxial traits. For example, $SR = AD_SD/(AD_SD + AB_SD)$.

E. QUANTITATIVE GENETIC ANALYSES

To estimate clonal values of genets from the phenotyped ramets, mixed-effects models were fit with lme4 (Bates et al., 2015) and the response, here a trait, was modelled as a function of the fixed effects of garden row and column position, and random effects of genet. A normal distribution was assumed for all traits except: disease ordinal 1 (2015), disease ordinal 1 and 2 (2016), SR, LR, and PR. To model non-normal responses of disease ordinal replicate values, four error distributions were fit to the data and compared with AIC using glmmADMB (Fournier et al., 2012; Skaug et al., 2016) and lme4, which include: (1) a standard mixed-effects model; (2) a zero-inflated negative binomial model with variance = $\mu(1 + \mu/k)$; (3) zero-inflated negative binomial model with variance = $\phi\mu$; and (4) a zero-inflated Poisson model. A zero-inflated Poisson model was used for the error distribution for disease ordinal 1 (2015) and (2016). A zero-inflated negative binomial error model with variance = $\mu(1 + \mu/k)$ was used for disease ordinal 2 (2016). For the SR, LR, and PR traits, the response was log-transformed and clonal values created with a standard mixed effects model using a normal error distribution.

To investigate how hybridization alters trait means and heritable variation, we used partial least squares regression (PLS) and estimated broad-sense heritability. PLS was performed in R (R Core Team, 2018) with the package mixOmics (Rohart et al., 2017) using canonical correlation where the X matrix was a column vector of the proportion of ancestry attributable to each species (determined by NewHybrids), and the Y matrix was a column vector of traits. To understand how backcrossing into *P. balsamifera* alters trait values, we plotted the filial generation estimated by NewHybrids against the trait as boxplots and performed Tukey's post-hoc tests to determine significance at $\alpha < 0.05$. Broad-sense heritability (H^2) was estimated with hybrids present and absent with MCMCglmm (Hadfield, 2010) by estimating the variance-covariance matrix of the fixed and random effects and the intercept. Models were run for 50,000 to 500,000 iterations until effective sample sizes of posterior parameters were above 1000. Normal distributions were assumed for continuous traits. Broad-sense heritability was estimated using the following equation:

$$H^2 = \frac{\sigma^2 \text{ genet}}{\sigma^2 \text{ genet} + \sigma^2 \text{ error}}$$

where σ^2 represent error attributable to position of the ramet in the garden and measurement error. The posterior mode and highest posterior density interval of the heritability estimate were reported.

To understand which traits correlated most strongly with the three disease phenotypes, we fit a MANOVA in R using the three disease phenotypes as a multivariate response and the remaining stomatal and ecophysiology traits as predictors. To test for selection trade-offs between growth, disease resistance, and stomatal ratio, we fit linear models in a path analysis framework. Disease resistance was calculated as -1 * D2". Traits were centered and standardized before regression models were fit. Model specifications are provided in Table 4. Each model was fit with three sets of data: hybrids absent, unadmixed *P. balsamifera* and *Tacamahaca* hybrids, and unadmixed *P. balsamifera* and *Aigeiros* hybrids. Evidence for trade-offs between

traits was considered present if the product of the slopes was negative (Schluter et al., 1991); similarly, selection conflicts were inferred if the product of the slopes from a trade-off were negative (Schluter et al., 1991). Significance testing of the observed regression coefficients was performed by generating a permuted distribution of regression coefficient products, and comparing the observed product to the distribution of permuted products. To generate permuted regression coefficient product distributions, the underlying trait data were permuted 1000 times and regression models were fit. The regression coefficient products were recorded, and a two-tailed probability test was used to generate a p-value for each observed regression coefficient product. Additionally, we performed a PCA of the three disease phenotypes with relative growth rate to decompose the relationship into orthogonal vectors. PC1 and PC2 were regressed against stomatal ratio to determine if the slopes from each set of hybrids were conflicting in sign, and hence, suggestive of a selection conflict on stomatal ratio in relation to growth and disease.

III. RESULTS

A. GENETIC ANCESTRY AND TRAIT VARIATION

Extensive backcrossing and hybridization was revealed from the NewHybrids analyses (Fig 1c, Table 2, Table S4). Our sample collection protocol was designed to target non-hybrid genotypes, thus the distribution of hybrids in our sample is less than what is expected on the landscape. Nevertheless, we observe hybrids at the F_1 to advanced generations backcrossing into *P. balsamifera* from *P. angustifolia*. Hybrids formed with *P. trichocarpa* were observed from the P1.F_1 generation and beyond, while *P. deltoides* hybrids were only observed at the F_1 generation.

Disease severity was measured across two years with two different ordinal scales. Distributions of all three disease severity phenotypes revealed a zero-inflated distribution, along with highly variable patterns of disease between BxB and hybrid genotypes (Fig. 1d). Zero-inflated distributions were observed for the underlying disease traits, and traits which incorporated adaxial stomata (Fig. S1). Section *Tacamahaca* hybrids exhibited decreased growth in comparisson to unadmixed *P. balsamifera* or the hybrids with a *Aigeiros* parent. The stomatal ratio was zero-inflated and the tail of had a median of 0.18 with a min. of 0.05 and a max. of 0.44. Hybrid genotypes, along with 43 of 315 unadmixed BxB individuals, had an elevated stomatal ratio. A PCA of the non-disease traits revealed stomata variation drives the principal axis of variation, while variation along PC2 was largely driven by of ecophysiology traits. Mapping hybrid cross type and disease presence or absence into the PC space revealed patterns of disease associated with negative values of PC1, an axis largely describing adaxial stomatal patterning (Fig. 1e). Segregation of the trait space was loosely clustered by the identity of the non-*balsamifera* parent (Fig. 1e).

As expected, hybridization altered trait means and variances (Table 1, Fig. S2, Fig. S3). Disease traits increased with increasing phylogenetic distance of the non-*balsamifera* parent, and transgressive segregation was observed for the adaxial and abaxial stomata traits as well as for Δ^{13}C in BxA hybrids (Fig. S2).

PLS analyses were conducted to investigate the effects of variation of the expected proportion of ancestry from each species (X matrix) on trait variation (Y matrix). The scalar product between pairs of vectors in the X and Y matrices indicate correlation between sets of variables. Using hierarchical clustering of the scalar products, we observed two large blocks: one characterized by high scalar product values between the ancestry proportions to SR, LR, PR, adaxial stomata, and the disease traits; and the

second block contained abaxial stomata, and ecophysiology traits with generally lower scalar product values to the ancestry proportions (Fig. 2).

In addition to shifting trait means, hybridization altered genotypic variance, resulting in increased heritability for the disease severity, SR, LR, PR, and adaxial stomatal patterning traits (Fig 2, Table S2). The H^2 for ecophysiology and abaxial stomatal patterning traits was less influenced by hybridization, and generally lower. As a whole, H^2 estimates ranged from 0.08 (CN) to 0.79 (SD_AD) (Fig 2).

Backcrossing into *P. balsamifera* decreased disease severity in advanced generation hybrids (Fig. 3a). Tukey's post-hoc tests indicated significant differences in disease severity between F_1, F_2, and P1.F_2 backcrosses to advanced generation backcrosses and unadmixed *P. balsamifera*. The stomatal ratio remained high among the filial generations and only decreased in unadmixed *P. balsamifera* (Fig. 3b). When accounting for the effect of SR on PC1 of disease, residuals were significantly different for the F_1 generation and remained uniform for all other filial generations (Fig. 3c). Growth was not significantly different among filial generations and was only significantly elevated in unadmixed *P. balsamifera* (Fig. 3d).

The effect of hybrid cross type on disease, stomatal patterning, and ecophysiology traits was explored with boxplots (Fig. S2). BxB genotypes generally had low disease, stomata patterning ratios, and adaxial stomatal patterning values. Patterns between ecophysiology traits were more nuanced. The effect of backcrossing on the traits was determined (Fig. S3), and in generally, stomatal patterning and disease traits demonstrated large variation between filial classes. Transgressive segregation in F_2 filial generation hybrids was observed for Δ^{13}C, C:N, and for CCI in P1.F_2 hybrids.

A MANOVA was fit using the three disease traits as the response and the remaining traits as predictors to model which traits best predicted variation of disease severity. stomatal ratio and growth were the most significant predictors (p-value < 0.001), followed by the stomata pore length ratio, adaxial stomata density, porosity ratio, and abaxial porosity (Table 3). Plotting the regression coefficients of each response revealed that multivariate disease traits did not always respond in the same direction to the predictors (Fig. 4). For example, the stomatal ratio had a positive regression coefficient to each of the disease responses ($\beta = 1.1, 0.5, 0.4$), while stomatal pore length ratio had one positive and two negative regression coefficients to the disease responses ($\beta = 0.7, -1.3, -0.6$).

B. SELECTION TRADE-OFFS AND CONFLICTS

To determine if there was evidence for evolutionary trade-offs in unadmixed and admixed populations, linear and multiple regression models were fit for two components of fitness, growth and disease resistance, and one metric trait, stomatal ratio. Trade-offs were differentially expressed if hybrids were present or absent from the analysis, and whether they involved *Tacamahaca* or *Aigeiros* hybrids (Table 4, Table S3). Disease resistance had a negative correlation with growth when hybrids were absent ($\beta = -0.18^{ns}$), and in the *Aigeiros* set ($\beta = -0.17^{*}$); however, in the *Tacamahaca* set, disease resistance had a positive relationship with growth ($\beta = 0.15^{ns}$). The positive slope in the *Tacamahaca* hybrids was due to the decreased disease resistance in the hybrid genotypes. For the multiple regression of SR on growth while including disease resistance, negative regression coefficients were found for all three data sets, but the regression coefficient was not significant in the *Aigeiros* data

set. Significant negative regression coefficients were found for all three data sets in the linear regression of stomatal ratio on disease resistance, indicating a decrease in the stomatal ratio increased disease resistance. The cumulative effect of both paths of stomatal ratio on growth was negative for the unadmixed *P. balsamifera* data set ($R_{SR,G} = -0.24$) and in the *Tacamahaca* data set ($R_{SR,G} = -0.40$), but closer to zero in the *Aigeiros* data set ($R_{SR,G} = -0.07$). The smaller value of the path analysis in *Aigeiros* hybrids may have indicated the trade-off was less severe.

Selection conflicts exist between pairs of traits if the product of their selection gradients are negative (Schluter et al., 1991). We observe a selection conflict between disease resistance and growth (β_1) and SR and growth (β_2) in the data set that includes the *Tacamahaca* and unadmixed *P. balsamifera* (Table 4). This selection conflict may indicate that selection for disease resistance at the expense of decreased growth cannot be achieved through selection for lower values of SR.

We can further view how hybridization reveals trade-offs in admixed and undadmixed populations by plotting stomatal ratio as a predictor to principal components reflecting the trade-off between growth and disease severity (Fig. 5). PC1 largely represents disease severity variance, while PC2 largely describes growth variance. Unadmixed *P. balsamifera* and *Tacamahaca* hybrids have a positive relationship to PC1, while poplars admixed with *P. deltoides* have a negative slope. Regressing stomatal ratio on PC2 reveals a slight positive relationship in BxB and BxT genotypes and negative slopes in BxA and BxD hybrids, although these are not statistically significant.

IV. DISCUSSION

We conducted a common garden study with naturally formed *Populus* hybrids to observe how hybridization alters trait value distributions, heritable variation, and the potential to reveal trade-offs and selection conflicts. We focused on growth, disease, and the stomatal ratio, as these traits contribute to fitness and were previously implicated in disease variation within unadmixed *P. trichocarpa* (McKown et al., 2014; McKown et al., 2019). These results indicate hybridization increases disease severity, decreases growth of hybrids formed from within-*Tacamahaca* crosses, and increases the stomatal ratio. Our results demonstrate increases in stomatal ratio are consistently correlated across years and measurement scales with an increase in disease severity. The negative correlation between stomatal ratio and disease resistance may be indicative of a locally adaptive trade-off evolved in the non-*balsamifera* parental species, which is still being expressed in the hybrids we sampled. The high H^2 of the stomatal ratio and its strong covariation to the proportion of *P. balsamifera* ancestry suggest selection could effectively reduce disease within a population by selecting for lower values of stomatal ratio, and, in this system, increased growth is a likely result. Although unadmixed *P. balsamifera* did experience disease, hybridization introduced more variation than was observed in unadmixed populations; demonstrating that hybridization studies can use the increased variance present in admixed populations to reveal trade-offs and selection conflicts that generations of natural selection has purged from unadmixed populations.

Given sufficient selection from pathogens and heritable variation, plant species will evolve an optimum along the growth-defense spectrum that maximizes their fitness based on the likelihood of pathogen exposure, physiological severity of the disease, and the cost of mounting a defense (Stearns, 1989; Schluter et al., 1991). That optimum can be locally adapted, change between populations within a species (e.g. northern versus southern populations of *P. trichocarpa*, McKown et al., 2014), as

well as evolve different adaptive combinations of traits between species. When hybrids are formed, misaligned growth-defense strategies expressed in a hybrid genotype can negatively impact its fitness through outbreeding depression (Goldberg et al., 2005), perhaps even in the presence of heterosis, as suggested by the increased disease of F_1 BxD hybrids we study here.

The effect of phylogenetic distance on these traits may be indirectly inferred from the distribution of traits arranged by hybrid cross type. Increasing the phylogentic distance of the non-*balsamifera* parent tended to increase disease severity and decrease growth. Although, the increased phylogenetic distance between *P. balsamifera* and *P. deltoides* likely induced heterosis for growth, but is accompanied by increased disease (Fig. 1d) and increased stomatal ratio; thereby revealing a growth-defense trade-off. Interestingly, the BxD hybrids do not have increased Δ^{13}C, which is partially an indicator of how closed stomata are, and analysis of the residuals from $D_{PC1} \sim SR$ indicate effects in addition to the stomatal ratio contribute to significantly elevated disease (Fig. 3). These results allow us to speculate that the increased disease in BxD F_1 hybrids may relate to a loss of resistance loci as a result of the accumulation of genetic incompatibilities, in addition to variance of stomatal patterning traits. While we do not have trait data for unadmixed *P. trichocarpa*, *P. angustifolia*, or *P. deltoides*, the growth-defense phenotypes in hybrids with ancestry from those species suggests different adaptive strategies from what has evolved in *P. balsamifera*. Common garden studies in *P. trichocarpa* have demonstrated that genotypes from Northern latitudes have more adaxial stomata, larger stomatal aperture pores, and increased carbon gain, but lower levels of defensive phenolic compounds and increased foliar pathogen disease (McKown et al., 2014). This suggests one fitness strategy, typified by *P. trichocarpa*, is to maximize growth while tolerating the negative effects of disease. Further research is needed to compare the growth-defense strategies of multiple unadmixed *Populus* species in a common environment.

In addition to increasing genetic variance, hybridization can disrupt co-adapted immune systems responses in host plants, possibly leading to increased disease susceptibility. Plant populations will typically evolve towards increased disease resistance with lower growth, or increased growth with lower disease resistance (Stearns, 1989; Schluter et al., 1991). In line with those expectation, we observe a negative relationship between disease resistance and growth in unadmixed *P. balsamifera* and *Aigerios* F_1 hybrids (Table 4). However, in *Tacamahaca* hybrids, we observe decreased disease resistance correlated with decreased growth. This correlation may be the result of negative physiological effects of increased pathogen presence on the host trees leading to a reduction in growth. Comparison of the slopes of G $\sim$ D and G $\sim$ SR indicate a selection conflict is present in *Tacamahaca* hybrids that have lower growth, decreased disease resistance, and increased stomatal ratio. One possible interpretation of the selection conflict is the positive slope between disease resistance and growth observed in *Tacamahaca* hybrids indicates that these populations cannot evolve towards one of the two optimal trait spaces along the growth-defense spectrum by decreasing stomatal ratio values, or by tolerating increased disease and instead investing more in growth.

The presence of amphistomy (having stomata on both leaf surfaces) as a result of hybridization raises interesting evolutionary consequences. Theoretical models of the benefits and costs of amphistomy indicate the increased efficiency of photosynthesis under amphistomy should lead to more species organizing their stomata on both surfaces (Muir, 2015). Yet, hypostomy (stomata only on the abaxial surface) predominates, particularly in trees and shrubs. Models which incorporate costs of amphistomy indicate a narrow range of optima, with few intermediate values of stomatal ratio (Muir, 2015). The results from this study

support theoretical conclusions that the costs of amphistomy are sufficiently high to constrain the available trait space in which plants evolve, and selection from pathogens likely induces a cost of amphistomy that is paid in the currency of fitness. Amphistomy is rare in *P. balsamifera*, which likely reflects the evolution of fitness optima that prioritizes defense over growth, which stands in contrast to northern populations of *P. trichocarpa* that have possibly evolved increase stomatal ratio to favor growth over defense (McKown et al., 2014; McKown et al., 2019).

The high heritability of disease severity, stomatal ratio, and the other adaxial stomata traits indicates selection could effectively purge genetic variance linked to disease susceptibility. Indeed, disease severity and stomata ratio are strongly correlated with the proportion of *P. balsamifera* ancestry (Fig. 2), and to each other (Table 3, Fig. 4), and have high heritabilities. Thus, we can predict that if pathogens exert a strong selective pressure on these populations, and if disease resistance is linked to low stomatal ratios (which our results indicate), selection will favor low stomatal ratio values. Unadmixed *P. balsamifera* have low stomatal ratio and high disease resistance, and it is likely that selection for low stomatal ratio values has occurred in this species.

The increased disease we observed in hybrid poplars may be a common feature of hybrid zones, and indeed, hybrid zones may even provide refuge for pathogens and pests (Whitham, 1989). For example, hybrids of *Salix eriocephala* and *S. serica* have a 3.5 fold increase in disease severity to *Melamposora* sp. and transgressively segregate for this trait (Roche and Fritz, 1998). Naturally formed F_1 *P. balsamifera* x *angustifolia* hybrids transgressively segregate for the number of galls per tree and back-crosses into *P. balsamifera* are even more susceptible to gall forming pests and have higher variance than F_1 or unadmixed parental species genotypes (Floate et al., 2016). Similar trends have been observed in animal hybrid zones, where F_1 and F_2 largemouth bass (*Micropterus salmoides*) have lower survival after inoculation with *Ranavirus* as a result of outbreeding depression (Goldberg et al., 2005).

The occurrence of multiple different species admixed with *P. balsamifera* allowed us to indirectly observe the effect of phylogenetic distance between parental species on trade-offs between growth and disease resistance, and to speculate on their importance in maintaining species barriers. Disease increased with phylogenetic distance of the non-*balsamifera* parent (Fig. 1, Fig. S1), and is ameliorated by back-crossing into *P. balsamifera* (Fig. 3). The evidence we present suggests shifts in stomatal ratio underlie much of the increase in disease; however, other studies point to the accumulation of genetic incompatibilities in hybrids as a cause of disease and disease-like symptoms which contribute to reproductive isolation and the maintenance of species barriers. Simulation studies of genetic incompatibilities have demonstrated that relatively few two-locus incompatibilities are required to maintain reproductive isolation in the presence of selection (Lindtke and Buerkle, 2015). Our finding of significant ancestry proportion effects on disease susceptibility suggests hybridization may also introduce genetic incompatibilities that disrupt the immune system. While any lethal combinations would have been filtered by selection in our sample, incompatibilities at loci in the innate or inducible immune system may persist into later life stages and filial generations, and could yield increased disease. Mapping these loci and tracking incompatibitilites in recombinant genotypes could test the hypothesis generated by the reduction of disease in recombinant genotypes that we observe (Fig. 3).

Despite the potential loss of fitness in hybrid genotypes, hybrid populations are ubiquitous in nature, and hybridization

represents an opportunity for the sharing of adaptive alleles evolved in one species to another (Chhatre et al., 2018; Suarez-Gonzalez et al., 2018c). Adaptive introgression of disease resistance loci has been documented in humans (Racimo et al., 2015) and *Helianthus annuus* (Whitney et al., 2006), among other taxa. Adaptive introgression between the accessions of *P. balsamifera* and *P. angustifolia* under investigation here has documented the introgression of genes principally associated with photoperiodic regulation, cold hardiness and terpene synthesis (Chhatre et al., 2018). Although Chhatre et al. (2018) did not find introgressed loci directly linked to disease, studies between *P. balsamifera* and *P. trichocarpa* have identified *R*-genes and disease-associated loci introgressing in both directions (Suarez-Gonzalez et al., 2018a).

By studying traits contributing to fitness, selective regimes can be identified within and between species. Hybridization introduces genetic variance, which can reveal misalignment of modules of linked traits within a hybrid population. Selection can fine tune linked traits, by selecting for increased disease resistance or increased growth, but not both. Here, we have studied hybrid populations formed from four species to observe an expanded trait space. We are able to predict how selection is likely to constrain this trait space to achieve reduced disease; namely, through a decrease in the stomatal ratio. These results demonstrate the important evolutionary and ecological effects of hybridization in plant-pathogen interactions. The different trade-offs we observed for growth, disease resistance, and stomatal traits, are likely due to the effect of misaligned growth-survival strategies that have evolved in each species, in addition to the effect of heterosis. Future research in this system will focus on using admixture mapping to identify genomic regions which underlie the disease resistance observed in *P. balsamifera* and the increased variance of disease severity in hybrids. Understanding the core growth-survival strategies that have evolved in each species will allow ecologists to place their findings of disease ecology in hybrid zones into a wider context, and should be undertaken by future researchers.

Cuticle micrographs are deposited on Dryad (doi:10.5061/dryad.kh2gv5f). Raw sequence reads are available on NCBI SRA (accession # SRP070954). NewHybrids filail call probabilities are provided in Supplementary Information S4a-c. KCF conceived the study, phenotyped accessions, performed the analyses, and wrote the manuscript. DN provided elemental and stable isotope data. SRK acquired plant material, phenotyped accessions, and provided extensive feedback on earlier drafts, phenotypes, and DNA sequences for study. Both authors read and approved the final manuscript.

V. TABLES

Table 1: Trait definitions, abbreviations, and the mean (μ) $\pm$ standard deviation (σ) of traits with hybrids present and absent.

Trait	Abbr.	Min.	Max	Hybrids present $\mu \pm \sigma$	Hybrids absent $\mu \pm \sigma$
Disease severity 2015 scale 1	D1'	0.30	5.95	1.43 $\pm$ 1.44	1.01 $\pm$ 0.90
Disease severity 2016 scale 1	D2'	0.02	3.83	0.35 $\pm$ 0.80	0.10 $\pm$ 0.34
Disease severity 2016 scale 2	D2"	0.04	2.99	0.23 $\pm$ 0.43	0.10 $\pm$ 0.19
Relative growth rate (cm)	G	15.96	53.94	27.63 $\pm$ 6.46	27.78 $\pm$ 6.55
Stomatal ratio	SR	0.00	0.44	0.06 $\pm$ 0.10	0.03 $\pm$ 0.06
Pore length ratio	LR	0.00	0.53	0.16 $\pm$ 0.22	0.09 $\pm$ 0.18
Porosity ratio	PR	0.00	0.43	0.05 $\pm$ 0.08	0.02 $\pm$ 0.05
Abaxial stomata density (mm^2)	SD_AB	130.22	301.51	219.57 $\pm$ 30.55	221.99 $\pm$ 27.71
Adaxial stomata density (mm^2)	SD_AD	0.00	153.89	16.18 $\pm$ 27.43	6.71 $\pm$ 15.71
Abaxial pore length (μm)	PL_AB	21.07	35.14	25.65 $\pm$ 1.78	25.72 $\pm$ 1.57
Adaxial pore length (μm)	PL_AD	0.002	34.75	7.63 $\pm$ 10.71	4.45 $\pm$ 9.01
Abaxial porosity	PO_AB	7.7e4	1.5e5	1.1e5 $\pm$ 1.1e3	1.1e5 $\pm$ 1.1e4
Adaxial porosity	PO_AD	0.00	7.3e4	6.2e3 $\pm$ 1.1e3	2.7e3 $\pm$ 6.5e3
Total porosity	TO_PO	8.2e4	1.7e5	1.2e5 $\pm$ 1.3e3	1.2 e5 $\pm$ 1.2e4
Carbon isotope discrimination (‰)	Δ^{13}C	20.49	25.23	22.72 $\pm$ 0.71	22.62 $\pm$ 0.62
Nitrogen isotope value (‰)	δ^{15}N	2.25	4.27	3.34 $\pm$ 0.35	3.32 $\pm$ 0.35
Carbon:Nitrogen	CN	36.13	45.03	39.50 $\pm$ 1.30	39.53 $\pm$ 1.28
Carbon (%)	C	45.40	48.98	47.62 $\pm$ 0.47	47.65 $\pm$ 0.45
Nitrogen (%)	N	1.2840	1.2844	1.2840 $\pm$ 0.0005	1.2840 $\pm$ 0.0005
Specific leaf area	SLA	11.04	14.11	12.32 $\pm$ 0.36	12.31 $\pm$ 0.36
Chlorophyll content index	CCI	19.61	38.41	27.40 $\pm$ 2.98	27.66 $\pm$ 3.09

Table 2: NewHybrids results. The Ref. non-*Pb* (0) and Ref. *Pb* (1) columns refer to the size of the reference populations from which segregating loci were selected. The remaning columns describe the sizes of the filial generations in unknown samples. Abbreviations: Ref., reference population; *Pb.*, *Populus balsamifera*.

Parental species	Ref. non-*Pb.* (0)	Ref. *Pb.* (1)	*Pb.*	F_1	F_2	P0-F_1	P1-F_1	P0-F_2	P1-F_2	P0-P0F_1	P1-P1F_1	P0-P0F_2	P1-P1F_2
P. balsamifera x *trichocarpa*	46	38	407	-	-	-	2	-	32	-	15	-	35
P. balsamifera x *angustifolia*	37	114	216	22	3	-	3	-	-	1	3	-	1
P. balsamifera x *deltoides*	32	38	369	15	-	-	-	-	-	-	-	-	-

Table 3: Output of MANOVA with three disease severity traits jointly modelled as the response. Significance indicated as *** P < 0.001; ** P < 0.01; * P < 0.05; . < 0.1.

	Pillai	approx F	Pr(>F)	sig. code
SR	0.62632	127.381	<2.2e-16	***
G	0.18223	16.935	5.768e-10	***
LR	0.06101	4.938	0.002427	**
SD_AB	0.03874	3.063	0.028933	*
PR	0.03513	2.767	0.042616	*
PO_AB	0.03364	2.646	0.049882	*
CCI	0.02965	2.323	0.075884	.
PL_AD	0.02780	2.173	0.091975	.
C	0.01949	1.511	0.212453	
SD_AD	0.01781	1.378	0.250319	
N	0.01688	1.305	0.273694	
PL_AB	0.01343	1.034	0.378196	
Δ^{13}C	0.00718	0.550	0.648664	
δ^{15}N	0.00695	0.532	0.660778	
CN	0.00601	0.460	0.710751	
PO_AD	0.00505	0.386	0.763368	
SLA	0.00020	0.015	0.997448	

Table 4: Trade-offs and selection conflicts inferred from linear and multiple regression models of three traits: D, disease resistance; G, relative growth rate; and SR, stomatal ratio. Negative regression coefficients (β_n) or path analysis ($R_{SR,G}$) indicate a trade-offs is present. The path analysis sums each independent path of the effect of SR on G: path 1, β_2; path 2, $\beta_3 * \beta_1$. Selection conflicts are inferred when the product of regression coefficients are negative (Schluter et al., 1991). The hybrids absent set includes only unadmixed *P. balsamifera*, and the *Tacamahaca* and *Aigeiros* data sets add hybrid individuals. β_1 was taken from model 1. Significance testing for selection conflicts was performed with permutation tests (Fig. S4). Significance indicated as *** P < 0.001; ** P < 0.01; * P < 0.05.

$$model\ 1 : G \sim \mu + \beta_1 D + \epsilon$$
$$model\ 2 : G \sim \mu + \beta_1 D + \beta_2 SR + \epsilon$$
$$model\ 3 : D \sim \mu + \beta_3 SR + \epsilon$$

Trade-offs

Data set	β_1	β_2	β_3	$R_{SR,G}$
Hybrids absent	-0.18	-0.30*	-0.30***	-0.24
Tacamahaca	0.15	-0.32***	-0.49***	-0.40
Aigeiros	-0.17*	-0.21	-0.82***	-0.07

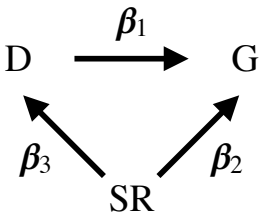

Selection conflicts

Data set	$\beta_1 * \beta_2$	$\beta_2 * \beta_3$
Hybrids absent	0.053*	0.089***
Tacamahaca	-0.050***	0.160***
Aigeiros	0.034**	0.168***

VI. FIGURES

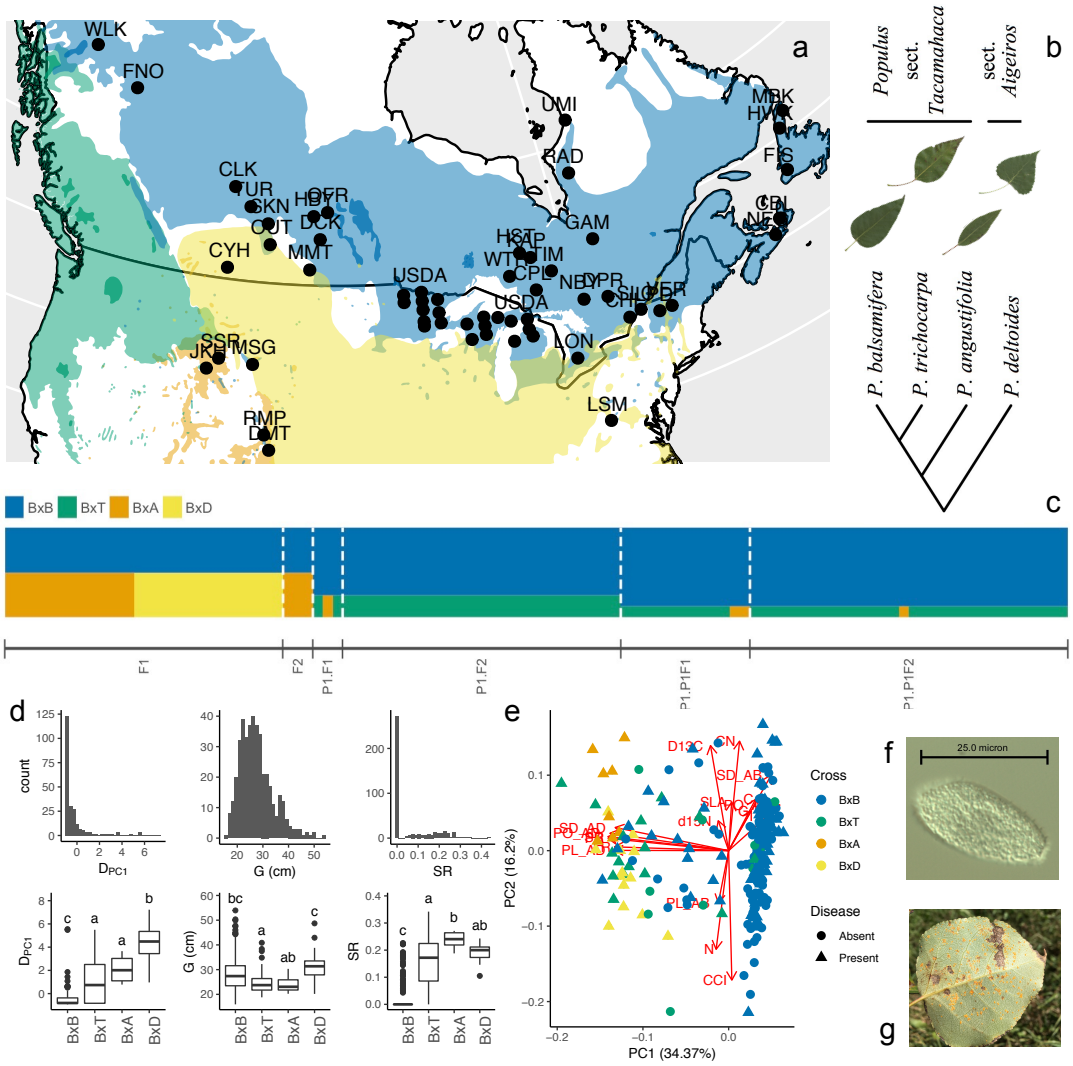

Figure 1: Summary of sample localities, phenotypes, and expected ancestry proportions for the trees under study. Sample locality map with the geographic ranges of four species of poplar: *P. balsamifera* (blue), *P. trichocarpa* (green), *P. angustifolia* (orange), and *P. deltoides* (yellow) (a). See Table S1 for population coordinates and samples sizes. The phylogenetic relationships of the four species under study are presented as a cladogram (b). The expected proportion of ancestry of hybrid genotypes was calculated from NewHybrid (Anderson and Thompson, 2002) estimates of filial generation (c). Histograms and box plots of three disease traits summarized by PC1 of a principle components analysis (D_{PC1}), relative growth rate (G), and stomatal ratio (SR). Tukey tests indicate significant differences at $\alpha < 0.05$. PCA of stomatal patterning and ecophysiology trait data. The presence or absence of disease and the hybrid cross type is mapped onto the points, but was not used to decompose variance of the traits in principle component space (e). Trait abbrevations in d and e are found in Table 1. Disease presence/absence calls in e were made from the eigenvalues for D_{PC1}, where PC1 eigenvalues greater than -0.8 were classified as diseased. Images of the uredospore (f) and disease sign of orange-yellow uredinia (g) of *Melampsora medusae* on an BxD hybrid.

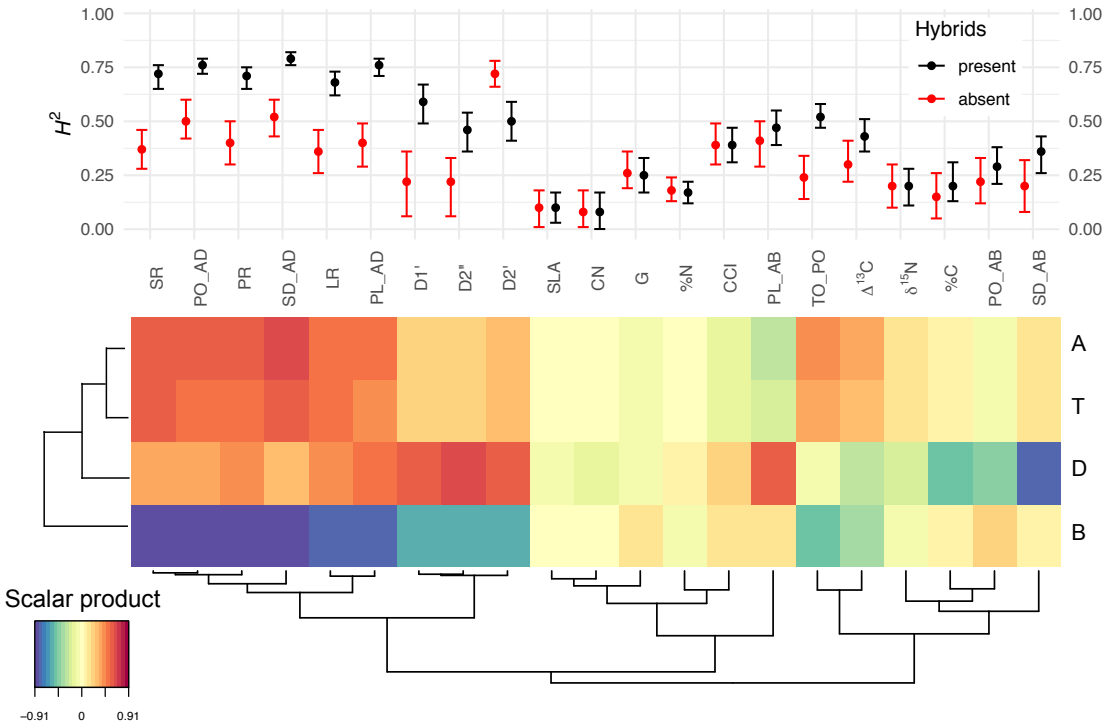

Figure 2: Results of partial least squares regression (PLS) of ancestry proportions and traits. B,D,T, and A represent vectors of the expected ancestry proportions for each individual estimated by NewHybrids (Table 2). The color ramp is the scalar product of variable loadings U' and V' from the X and Y matrices, respectively, indicating the correlation between pairs of vectors. Broad-sense heritability (H^2) estimates for each trait are given from data sets with hybrids present (black) and absent (red). 95% credible intervals indicated as whiskers. See text for PLS and H^2 estimation details and Table S2 for H^2 estimates.

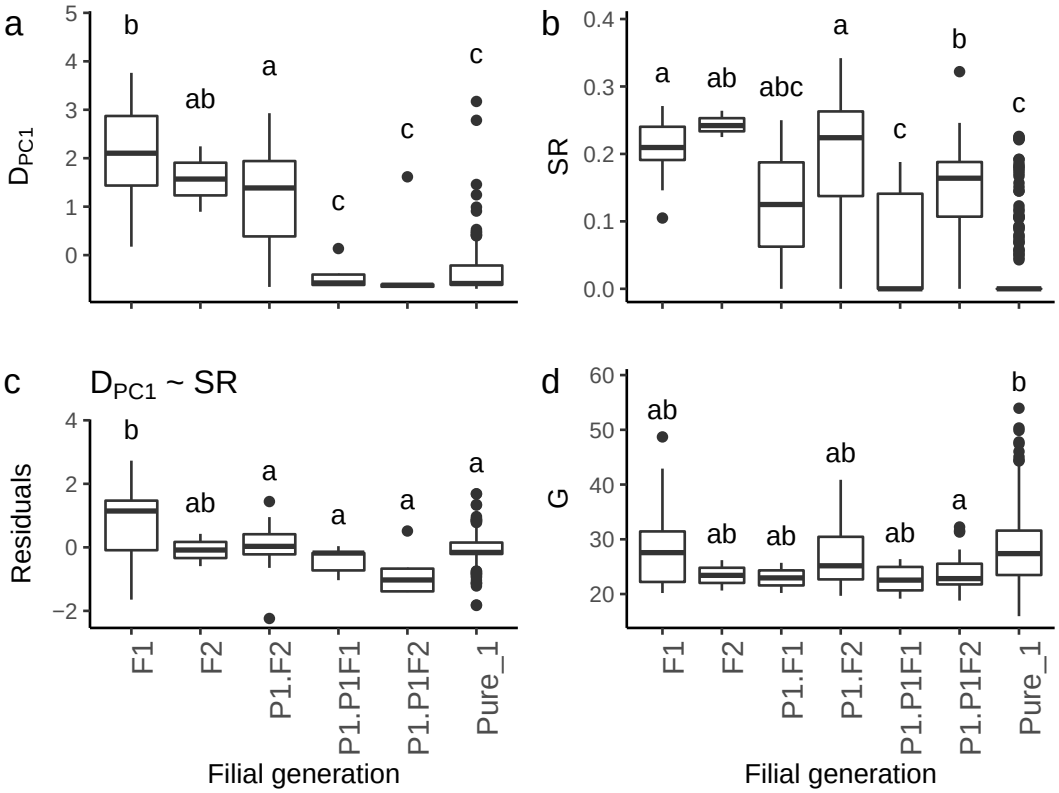

Figure 3: Backcrossing into *P. balsamifera* decreases disease (D_{PC1}) (a) and the stomatal ratio (SR) (b). When accounting for the effect of SR on disease, residual variance decreases from F_1 to F_n generations and unadmixed *P. balsamifera* (c). Growth is uniform across the filial generations (d). Differences in Tukey's post-hoc tests for significance (p-value < 0.05) indicated by letter.

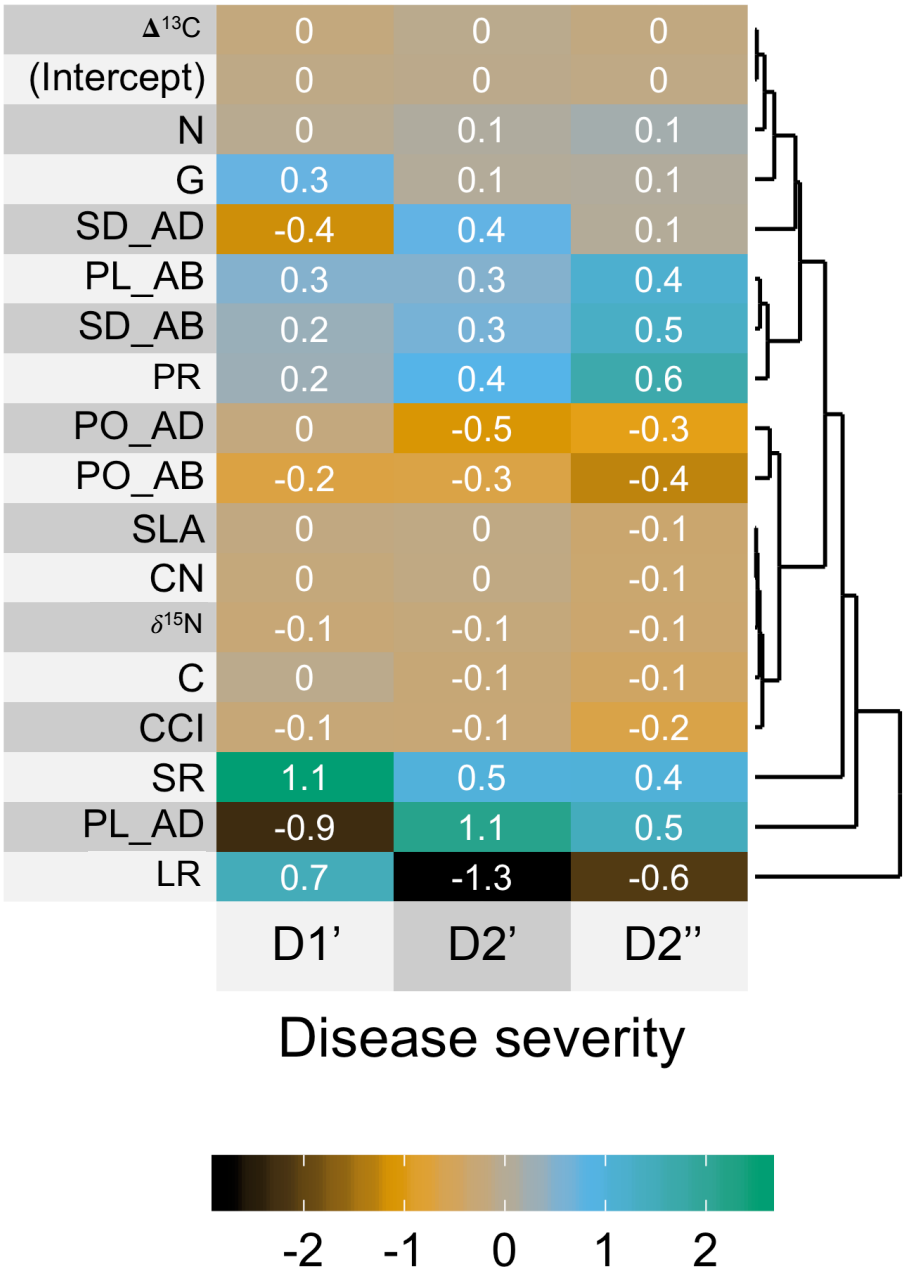

Figure 4: MANOVA regression coefficient heat map.

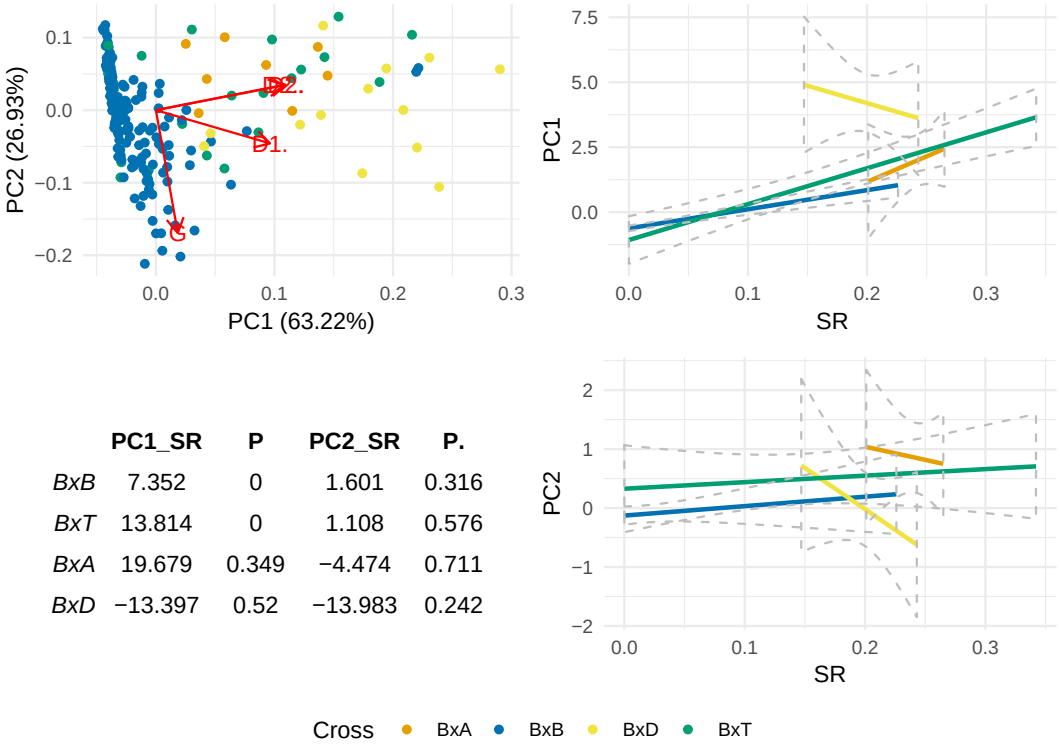

	PC1_SR	P	PC2_SR	P.
BxB	7.352	0	1.601	0.316
BxT	13.814	0	1.108	0.576
BxA	19.679	0.349	−4.474	0.711
BxD	−13.397	0.52	−13.983	0.242

Figure 5: Regression of stomatal ratio onto principal components 1 and 2 of disease severity and growth. Regression coefficients and significance indicated in panel with table.

References

Allen, E, B Hazen, H Hoch, Y Kwon, G Leinhos, R Staples, M Stumpf, B Terhune, et al. (1991). "Appressorium formation in response to topographical signals by 27 rust species." In: *Phytopathology* 81.3, pp. 323–331.

Altizer, S, R Bartel, and BA Han (2011). "Animal migration and infectious disease risk". In: *science* 331.6015, pp. 296–302.

Anderson, E and E Thompson (2002). "A model-based method for identifying species hybrids using multilocus genetic data". In: *Genetics* 160.3, pp. 1217–1229.

Bailey, JK, R Deckert, JA Schweitzer, BJ Rehill, RL Lindroth, C Gehring, and TG Whitham (2005). "Host plant genetics affect hidden ecological players: links among *Populus*, condensed tannins, and fungal endophyte infection". In: *Canadian Journal of Botany* 83.4, pp. 356–361.

Bates, D, M Mächler, B Bolker, and S Walker (2015). "Fitting Linear Mixed-Effects Models Using lme4". In: *Journal of Statistical Software* 67.1, pp. 1–48.

Browning, BL, Y Zhou, and SR Browning (2018). "A one-penny imputed genome from next-generation reference panels". In: *The American Journal of Human Genetics* 103.3, pp. 338–348.

Bruns, EL, J Antonovics, and M Hood (2018). "Is there a disease-free halo at species range limits? The co-distribution of anther-smut disease and its host species". In: *Journal of Ecology*.

Cai, Q, L Qiao, M Wang, B He, FM Lin, J Palmquist, SD Huang, and H Jin (2018). "Plants send small RNAs in extracellular vesicles to fungal pathogen to silence virulence genes". In: *Science* 360.6393, pp. 1126–1129.

Chandran, D, J Rickert, Y Huang, MA Steinwand, SK Marr, and MC Wildermuth (2014). "Atypical E2F transcriptional repressor DEL1 acts at the intersection of plant growth and immunity by controlling the hormone salicylic acid". In: *Cell host & microbe* 15.4, pp. 506–513.

Chhatre, VE, LM Evans, SP DiFazio, and SR Keller (2018). "Adaptive introgression and maintenance of a trispecies hybrid complex in range-edge populations of *Populus*". In: *Molecular ecology*.

Christe, C, KN Stölting, L Bresadola, B Fussi, B Heinze, D Wegmann, and C Lexer (2016). "Selection against recombinant hybrids maintains reproductive isolation in hybridizing *Populus* species despite F1 fertility and recurrent gene flow". In: *Molecular Ecology* 25.11, pp. 2482–2498.

Craine, JM, AJ Elmore, MP Aidar, M Bustamante, TE Dawson, EA Hobbie, A Kahmen, MC Mack, KK McLauchlan, A Michelsen, et al. (2009). "Global patterns of foliar nitrogen isotopes and their relationships with climate, mycorrhizal fungi, foliar nutrient concentrations, and nitrogen availability". In: *New Phytologist* 183.4, pp. 980–992.

Danecek, P, A Auton, G Abecasis, CA Albers, E Banks, MA DePristo, RE Handsaker, G Lunter, GT Marth, ST Sherry, et al. (2011). "The variant call format and VCFtools". In: *Bioinformatics* 27.15, pp. 2156–2158.

Dangl, JL and JD Jones (2001). "Plant pathogens and integrated defence responses to infection". In: *nature* 411.6839, p. 826.

DiFazio, SP, GT Slavov, and CP Joshi (2011). "*Populus*: a premier pioneer system for plant genomics". In: Enfield, NH: Science Publishers, pp. 1–28.

Dowkiw, A and C Bastien (2004). "Characterization of two major genetic factors controlling quantitative resistance to *Melampsora larici-populina* leaf rust in hybrid poplars: strain specificity, field expression, combined effects, and relationship with a defeated qualitative resistance gene". In: *Phytopathology* 94.12, pp. 1358–1367.

Eckenwalder, JE (1996). "Systematics and evolution of Populus". In: *Biology of Populus and its implications for management and conservation*. Ed. by R Stettler, T Bradshaw, P Heilman, and T Hinckley. Ottawa: NRC Research Press. Chap. 1, pp. 7–32.

Ellstrand, NC and KA Schierenbeck (2000). "Hybridization as a stimulus for the evolution of invasiveness in plants?" In: *Proceedings of the National Academy of Sciences* 97.13, pp. 7043–7050.

Elshire, RJ, JC Glaubitz, Q Sun, JA Poland, K Kawamoto, ES Buckler, and SE Mitchell (2011). "A robust, simple genotyping-by-sequencing (GBS) approach for high diversity species". In: *PloS one* 6.5, e19379.

Evans, LM, GT Slavov, E Rodgers-Melnick, J Martin, P Ranjan, W Muchero, AM Brunner, W Schackwitz, L Gunter, JG Chen, et al. (2014). "Population genomics of *Populus trichocarpa* identifies signatures of selection and adaptive trait associations". In: *Nature genetics* 46.10, p. 1089.

Farquhar, GD, MH O'Leary, and JA Berry (1982). "On the relationship between carbon isotope discrimination and the intercellular carbon dioxide concentration in leaves". In: *Functional Plant Biology* 9.2, pp. 121–137.

Feau, N, DL Joly, and RC Hamelin (2007). "Poplar leaf rusts: model pathogens for a model tree". In: *Botany* 85.12, pp. 1127–1135.

Fetter, KC, S Eberhardt, RS Barclay, S Wing, and SR Keller (2019). "StomataCounter: a neural network for automatic stomata identification and counting". In: *New Phytologist* 223.3, pp. 1671–1681.

Floate, KD, J Godbout, MK Lau, N Isabel, and TG Whitham (2016). "Plant–herbivore interactions in a trispecific hybrid swarm of *Populus*: assessing support for hypotheses of hybrid bridges, evolutionary novelty and genetic similarity". In: *New Phytologist* 209.2, pp. 832–844.

Fournier, DA, HJ Skaug, J Ancheta, J Ianelli, A Magnusson, MN Maunder, A Nielsen, and J Sibert (2012). "AD Model Builder: using automatic differentiation for statistical inference of highly parameterized complex nonlinear models". In: *Optim. Methods Softw.* 27, pp. 233–249.

Glaubitz, JC, TM Casstevens, F Lu, J Harriman, RJ Elshire, Q Sun, and ES Buckler (2014). "TASSEL-GBS: a high capacity genotyping by sequencing analysis pipeline". In: *PloS one* 9.2, e90346.

Goldberg, TL, EC Grant, KR Inendino, TW Kassler, JE Claussen, and DP Philipp (2005). "Increased infectious disease susceptibility resulting from outbreeding depression". In: *Conservation Biology* 19.2, pp. 455–462.

Gonzales-Vigil, E, CA Hefer, ME von Loessl, J La Mantia, and SD Mansfield (2017). "Exploiting natural variation to uncover an alkene biosynthetic enzyme in poplar". In: *The Plant Cell*, tpc–00338.

Goulet, BE, F Roda, and R Hopkins (2017). "Hybridization in plants: old ideas, new techniques". In: *Plant physiology* 173.1, pp. 65–78.

Hadfield, JD (2010). “MCMC Methods for Multi-Response Generalized Linear Mixed Models: The MCMCglmm R Package”. In: *Journal of Statistical Software* 33.2, pp. 1–22.

Kliebenstein, DJ (2016). “False idolatry of the mythical growth versus immunity tradeoff in molecular systems plant pathology”. In: *Physiological and Molecular Plant Pathology* 95, pp. 55–59.

La Mantia, J, J Klápště, YA El-Kassaby, S Azam, RD Guy, CJ Douglas, SD Mansfield, and R Hamelin (2013). “Association analysis identifies Melampsora× columbiana poplar leaf rust resistance SNPs”. In: *PLoS One* 8.11, e78423.

LeBoldus, JM, N Isabel, KD Floate, P Blenis, and BR Thomas (2013). “Testing the ‘hybrid susceptibility’and ‘phenological sink’ hypotheses using the *P. balsamifera–P. deltoides* hybrid zone and Septoria leaf spot [*Septoria musiva*]”. In: *PloS one* 8.12, e84437.

Li, H and R Durbin (2009). “Fast and accurate short read alignment with Burrows–Wheeler transform”. In: *bioinformatics* 25.14, pp. 1754–1760.

Lindtke, D and CA Buerkle (2015). “The genetic architecture of hybrid incompatibilities and their effect on barriers to introgression in secondary contact”. In: *Evolution* 69.8, pp. 1987–2004.

Mallet, J (2007). “Hybrid speciation”. In: *Nature* 446.7133, p. 279.

Martinsen, GD, TG Whitham, RJ Turek, and P Keim (2001). “Hybrid populations selectively filter gene introgression between species”. In: *Evolution* 55.7, pp. 1325–1335.

McKown, AD, RD Guy, L Quamme, J Klápště, J La Mantia, C Constabel, YA El-Kassaby, RC Hamelin, M Zifkin, and M Azam (2014). “Association genetics, geography and ecophysiology link stomatal patterning in *Populus trichocarpa* with carbon gain and disease resistance trade-offs”. In: *Molecular ecology* 23.23, pp. 5771–5790.

McKown, AD, J Klápště, RD Guy, OR Corea, S Fritsche, J Ehlting, YA El-Kassaby, and SD Mansfield (2019). “A role for SPEECHLESS in the integration of leaf stomatal patterning with the growth vs disease trade-off in poplar.” In: *The New phytologist*.

Melotto, M, W Underwood, J Koczan, K Nomura, and SY He (2006). “Plant stomata function in innate immunity against bacterial invasion”. In: *Cell* 126.5, pp. 969–980.

Messina, FJ, SL Durham, JH Richards, and DE McArthur (2002). “Trade-off between plant growth and defense? A comparison of sagebrush populations”. In: *Oecologia* 131.1, pp. 43–51.

Muir, CD (2015). “Making pore choices: repeated regime shifts in stomatal ratio”. In: *Proceedings of the Royal Society B: Biological Sciences* 282.1813, p. 20151498.

Obeso, JR (2002). “The costs of reproduction in plants”. In: *New Phytologist* 155.3, pp. 321–348.

Pinon, J and P Frey (2005). “Interactions between poplar clones and *Melampsora* populations and their implications for breeding for durable resistance”. In: *Rust Diseases of Willow and Poplar*. Ed. by MH Pei and AR McCracken. Wallingford, UK: CABI, pp. 139–154.

R Core Team (2018). *R: A Language and Environment for Statistical Computing*. R Foundation for Statistical Computing. Vienna, Austria.

Racimo, F, S Sankararaman, R Nielsen, and E Huerta-Sánchez (2015). "Evidence for archaic adaptive introgression in humans". In: *Nature Reviews Genetics* 16.6, p. 359.

Raven, PH and Zy Wu (1999). *Flora of China. 4, Cycadaceae Through Fagaceae*. Science Press.

Roche, B and R Fritz (1998). "Effects of host plant hybridization on resistance to willow leaf rust caused by *Melampsora* sp." In: *European Journal of Forest Pathology* 28.4, pp. 259–270.

Rohart, F, B Gautier, A Singh, and KA Lê Cao (2017). "mixOmics: An R package for 'omics feature selection and multiple data integration". In: *PLoS computational biology* 13.11, e1005752.

Schluter, D, TD Price, and L Rowe (1991). "Conflicting selection pressures and life history trade-offs". In: *Proc. R. Soc. Lond. B* 246.1315, pp. 11–17.

Schneider, CA, WS Rasband, and KW Eliceiri (2012). "NIH Image to ImageJ: 25 years of image analysis". In: *Nature methods* 9.7, p. 671.

Skaug, H, D Fournier, B Bolker, A Magnusson, and A Nielsen (2016). *Generalized Linear Mixed Models using 'AD Model Builder'*. R package version 0.8.3.3.

Stearns, SC (1989). "Trade-offs in life-history evolution". In: *Functional ecology* 3.3, pp. 259–268.

Suarez-Gonzalez, A, CA Hefer, C Lexer, QC Cronk, and CJ Douglas (2018a). "Scale and direction of adaptive introgression between black cottonwood (*Populus trichocarpa*) and balsam poplar (*P. balsamifera*)". In: *Molecular ecology* 27.7, pp. 1667–1680.

Suarez-Gonzalez, A, CA Hefer, C Lexer, CJ Douglas, and QC Cronk (2018b). "Introgression from *Populus balsamifera* underlies adaptively significant variation and range boundaries in *P. trichocarpa*". In: *New Phytologist* 217.1, pp. 416–427.

Suarez-Gonzalez, A, C Lexer, and QC Cronk (2018c). "Adaptive introgression: a plant perspective". In: *Biology letters* 14.3, p. 20170688.

Tian, D, M Traw, J Chen, M Kreitman, and J Bergelson (2003). "Fitness costs of R-gene-mediated resistance in *Arabidopsis thaliana*". In: *Nature* 423.6935, p. 74.

Tuskan, GA et al. (2006). "The genome of black cottonwood, *Populus trichocarpa* (Torr. & Gray)". In: *science* 313.5793, pp. 1596–1604.

Ullah, C, CJ Tsai, SB Unsicker, L Xue, M Reichelt, J Gershenzon, and A Hammerbacher (2018). "Salicylic acid activates poplar defense against the biotrophic rust fungus *Melampsora larici-populina* via increased biosynthesis of catechin and proanthocyanidins". In: *New Phytologist*.

Van Kraayenoord, C, G Laundon, and A Spiers (1974). "Poplar rusts invade New Zealand." In: *Plant disease reporter* 58.5, pp. 423–427.

Wang, ZY (2012). “Brassinosteroids modulate plant immunity at multiple levels”. In: *Proceedings of the National Academy of Sciences* 109.1, pp. 7–8.

White, J, B Vaughn, and S Michel (2011). “Stable Isotopic Composition of Atmospheric Carbon Dioxide (13C and 18O) from the NOAA ESRL Carbon Cycle Cooperative Global Air Sampling Network, 1990–2014, Version: 2015-10-26.” In: *University of Colorado, Institute of Arctic and Alpine Research (INSTAAR)*.

Whitham, TG (1989). “Plant hybrid zones as sinks for pests”. In: *Science*, pp. 1490–1493.

Whitney, KD, RA Randell, and LH Rieseberg (2006). “Adaptive introgression of herbivore resistance traits in the weedy sunflower *Helianthus annuus*”. In: *The American Naturalist* 167.6, pp. 794–807.

SUPPORTING INFORMATION

Table S3: Model output for trade-off regressions for the unadmixed BxB set (top), *Populus* sect. *Tacamahaca* (middle), and *P.* sect. *Aigeiros* (bottom) data sets. Significance indicated as *** P < 0.001; ** P < 0.01; * P < 0.05.

Hybrids absent

Variable	Statistic	Model 1	Model 2	Model 3
(Intercept)	Estimate	0.316***	0.225**	0.168***
	Std Err	[0.081]	[0.093]	[0.036]
D	Estimate	-0.179	-0.296*	
	Std Err	[0.150]	[0.160]	
SR	Estimate		-0.295**	-0.300***
	Std Err		[0.138]	[0.053]
	N	239	232	234
	R2	0.006	0.025	0.121
	adj R2	0.002	0.017	0.117
	AIC	698.750	678.857	266.631

Tacamahaca set

Variable	Statistic	Model 1	Model 2	Model 3
(Intercept)	Estimate	0.117*	0.114*	0.068*
	Std Err	[0.060]	[0.060]	[0.036]
D	Estimate	0.153*	-0.090	
	Std Err	[0.080]	[0.098]	
SR	Estimate		-0.324***	-0.492***
	Std Err		[0.080]	[0.038]
	N	294	286	288
	R2	0.013	0.067	0.367
	adj R2	0.009	0.060	0.365
	AIC	846.300	812.621	525.122

Aigeiros set

Variable	Statistic	Model 1	Model 2	Model 3
(Intercept)	Estimate	0.314***	0.261***	-0.144***
	Std Err	[0.066]	[0.076]	[0.051]
D	Estimate	-0.165**	-0.256***	
	Std Err	[0.074]	[0.093]	
SR	Estimate		-0.205	-0.820***
	Std Err		[0.126]	[0.068]
	N	252	245	247
	R2	0.020	0.030	0.372
	adj R2	0.016	0.022	0.369
	AIC	737.204	719.189	537.947

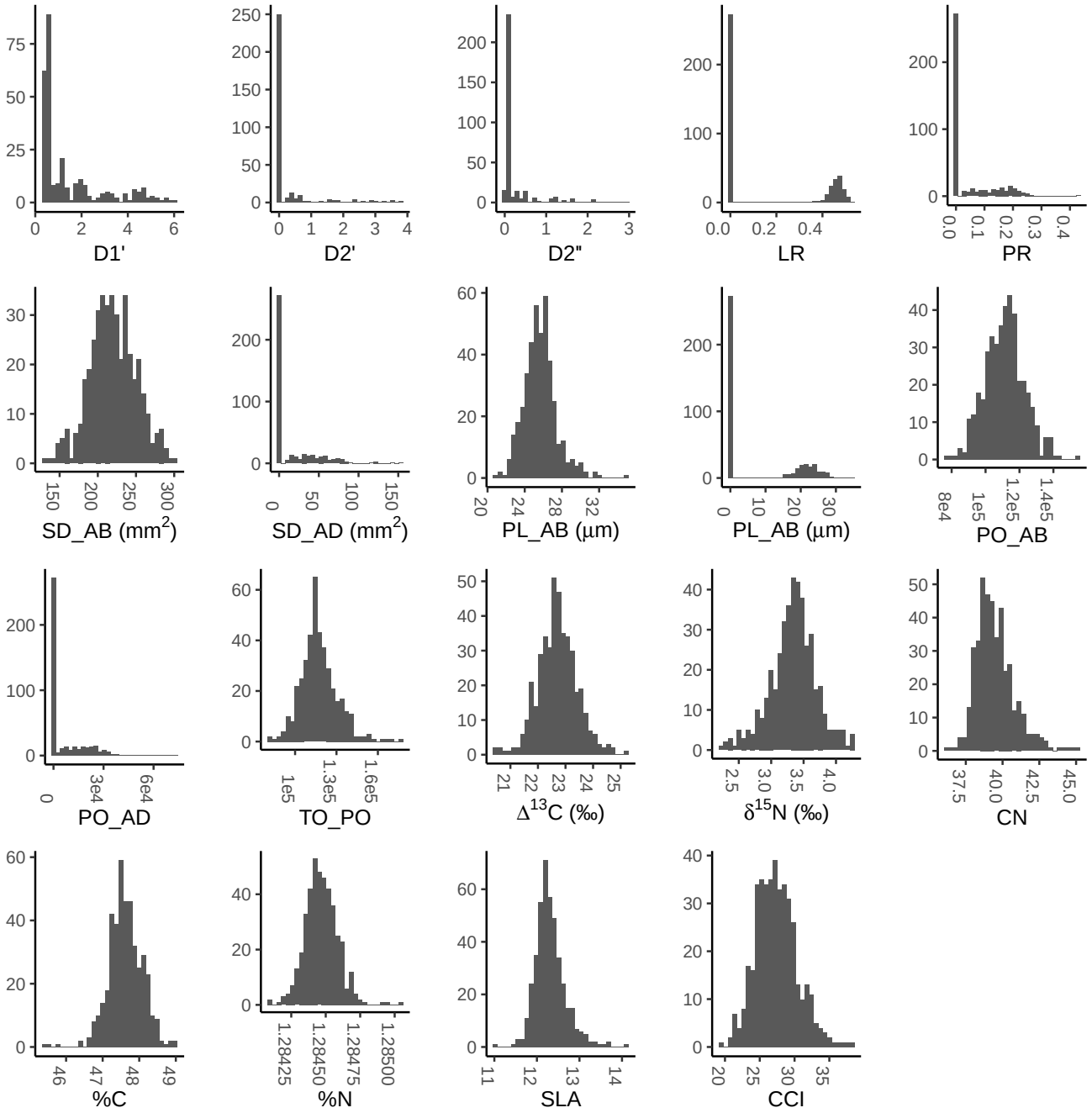

Figure S1: Distribution of clonal values. See Table 1 for trait abbreviations.

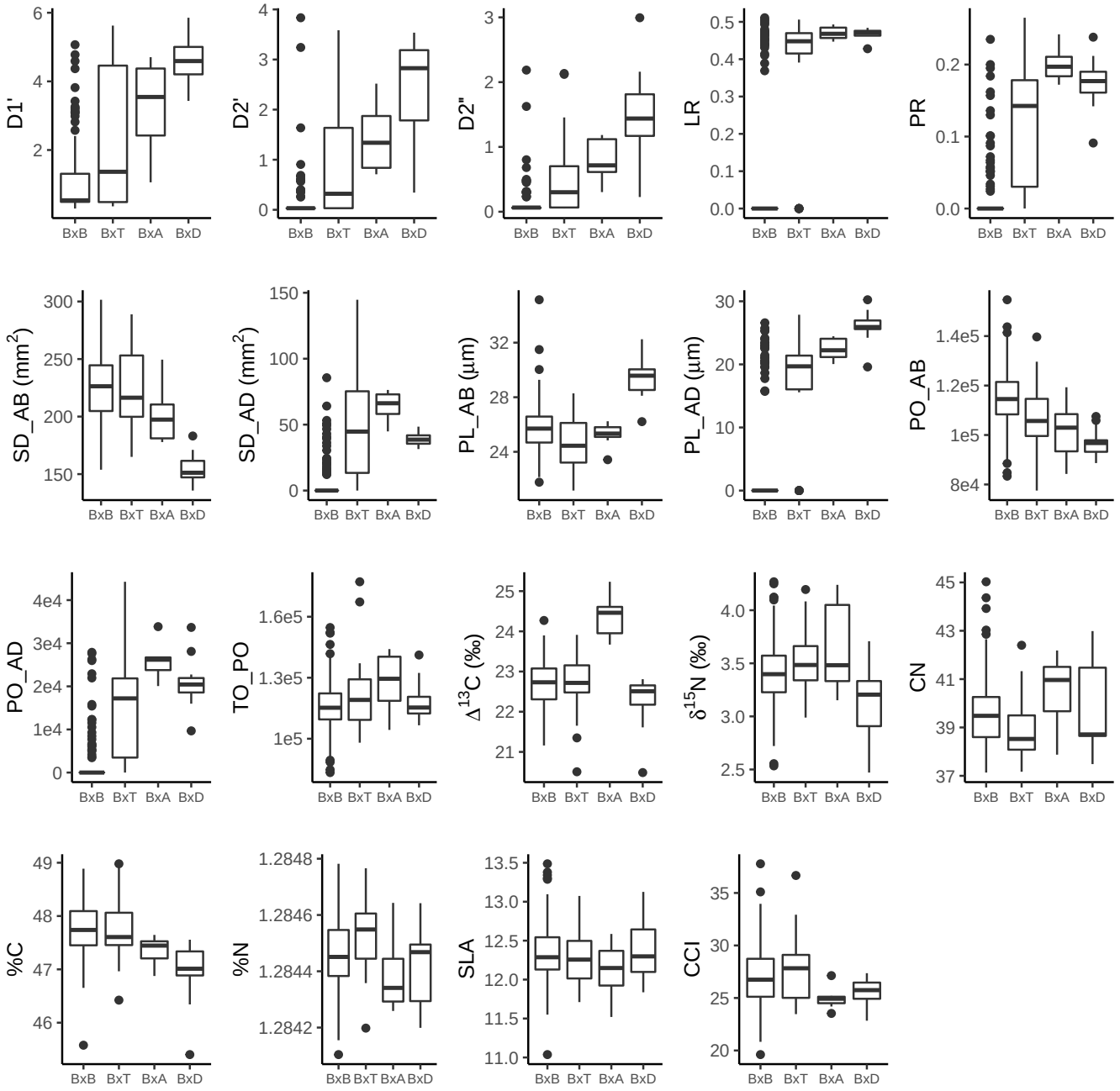

Figure S2: Variation of traits by cross type. See Table 1 for trait abbreviations.

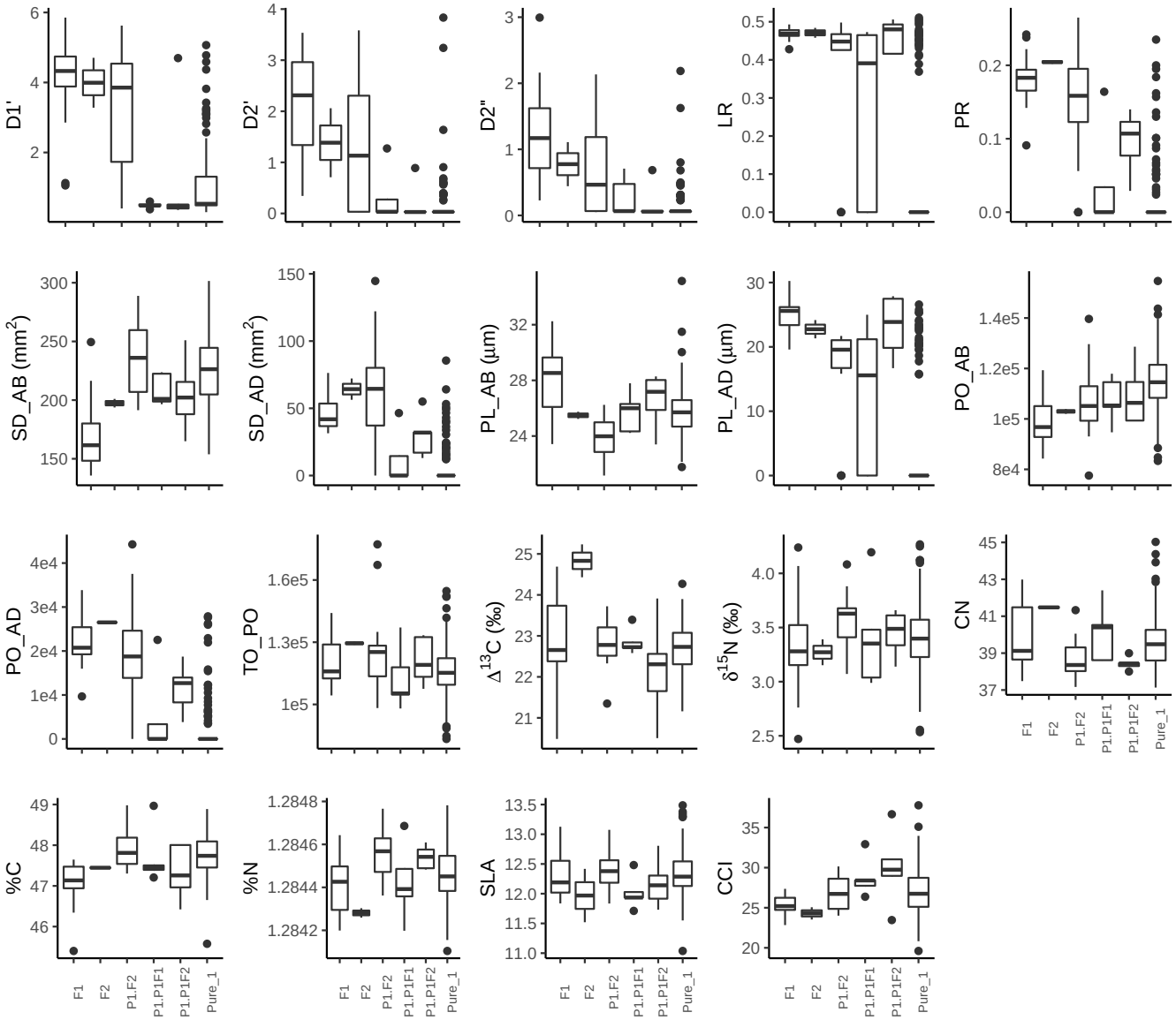

Figure S3: Variation of traits by filial generation. See Table 1 for trait abbreviations.

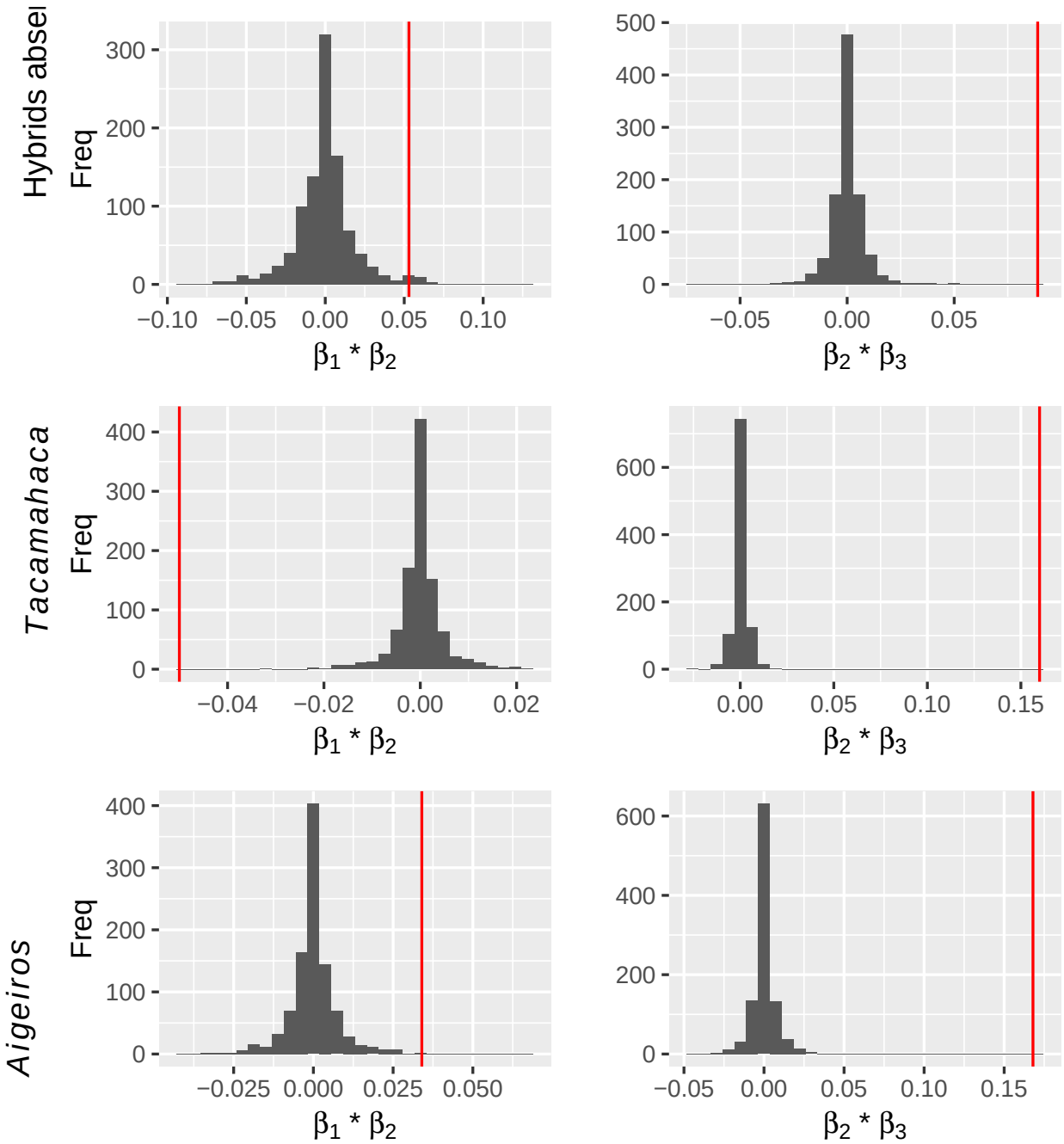

Figure S4: Permutation tests for significance of selection conflict products. The product of the regression coefficients for each pair of traits was estimated 1000 times with permuted data (grey distribution). The observed product is considered significant if its value is more extreme than the permuted distribution at $\alpha/2 = 0.025$. See Table 4 for results.